AJNR

Solitary fibrous tumor of the paranasal sinuses: CT and MR appearance.

T A Kim, J A Brunberg, J P Pearson and D A Ross

This information is current as of August 22, 2025.

Solitary Fibrous Tumor of the Paranasal Sinuses: CT and MR Appearance

Thomas A. Kim, James A. Brunberg, Jeffrey P. Pearson, and Donald A. Ross

Summary: We describe the CT and MR appearance of a solitary fibrous tumor of the paranasal sinuses with intracranial invasion. The tumor was hypointense on T2-weighted MR images and had a large calcific component that proved to be reactive remodeling of native bone.

Index terms: Paranasal sinuses, neoplasms

Solitary fibrous tumor, formerly known as *localized fibrous mesothelioma* or *benign fibrous mesothelioma*, is an uncommon neoplasm that typically presents as a pleura-based mass. In rare instances, the tumor may arise at an extrapleural site.

Case Report

A 69-year-old woman had a 6-month history of unilateral right-sided nasal obstruction and intermittent epistaxis with no visual dysfunction, headache, dysphagia, weight loss, or history of trauma.

Computed tomography (CT) showed a large mass arising from the superior aspect of the nasal cavity with extension posteriorly into the nasopharynx. Superiorly, the mass extended into the frontal sinuses and into the anterior cranial fossa through the cribriform plate as well as the roof of the ethmoidal sinus and the right orbit. The mass contained large, irregular areas of bone density centered at the ethmoidal sinuses. A small segment of tumor extended into the right orbit from the right ethmoidal sinus with destruction of the right lamina papyracea. The mass showed nearly homogeneous contrast enhancement (Fig 1A–C).

Magnetic resonance (MR) imaging at 1.5 T revealed a large soft-tissue mass within the nasopharynx, nasal cavity, right and left ethmoidal sinuses, and right sphenoidal sinuses, with extension into the right frontal sinus and the anterior cranial fossa. The intracranial portion of the mass, measuring $5.0 \times 3.8 \times 5.3$ cm, was associated with compression and posterior displacement of the frontal horns and of the genu and rostrum of the corpus callosum. There was a 1.0-cm shift of the interhemispheric fissure to the left (Fig 1D–H). The intracranial and nasopharyngeal portions of the mass were slightly inhomogeneous in signal intensity but were isointense with gray matter on T1-weighted images (550/16 [repetition time/echo time]) and hypointense relative to gray matter on spin-density (4848/18 effective) and T2-weighted (4848/90 effective) images. The mass showed a prominent and slightly inhomogeneous pattern of enhancement after intravenous injection of gadopentetate dimeglumine.

Craniofacial resection was performed via a combined bifrontal craniotomy and transfacial approach. The intradural tumor was resected first. The tumor was firm and encapsulated but the adjacent brain was soft and friable. The invaded bone of the frontal floor was resected en bloc along with the nasal portion of the tumor.

Gross pathologic examination revealed a dense rubbery white multinodular polypoid neoplasm, some of which was covered by sinus mucosa. One fragment consisted of bone surrounded and infiltrated by neoplasm. Microscopically, the tumor was composed of spindle cells with fine nuclear chromatin, inconspicuous nucleoli, and cytoplasm that was indistinct and eosinophilic. The cells were arranged haphazardly in a dense collagenous background (Fig 1I). The majority of the neoplasm had no organization and alternated between sclerotic hypocellular and hypercellular regions (Fig 1J). In foci, the neoplasm formed interlacing fascicles similar to those seen in low-grade fibrosarcomas, but mitotic figures were scarce, less than one per 50 high-power fields, and necrosis was absent. Sections through the portion of tumor containing a large central bone mass showed reactive remodeling of mature lamellar bone with regular cement lines, haversian canals, and fatty marrow that was extensively infiltrated by tumor (Fig 1K). This was native bone involved by tumor and not metaplastic or neoplastic bone. Immunohistochemical testing showed the neoplastic cells were positive for CD34 (Fig 1L) and negative for cytokeratins.

After surgery, the patient had no neurologic deficits until her steroids were tapered off 1 week after surgery, when bifrontal brain edema developed. This resolved over
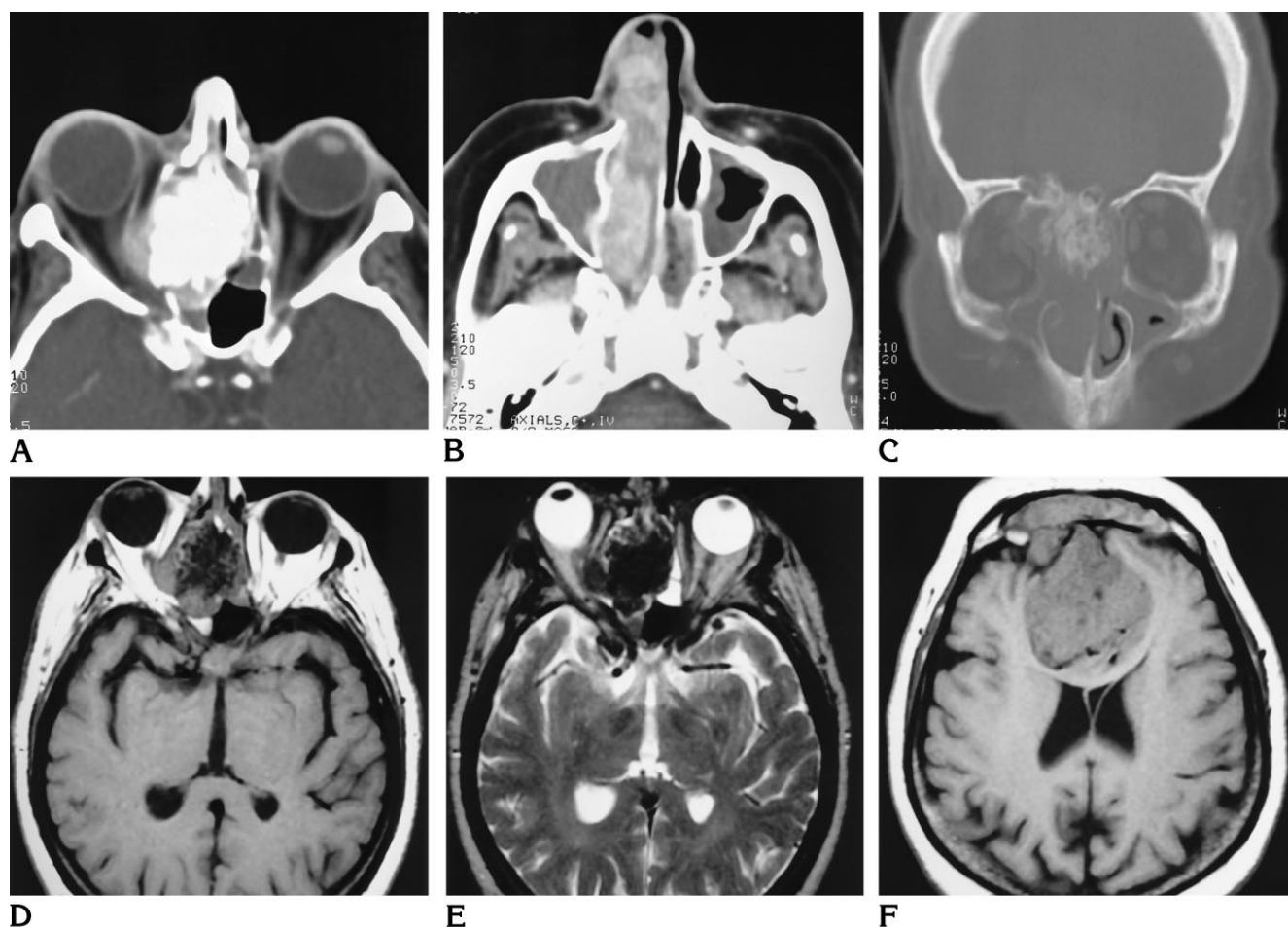
Fig 1. Sixty-nine-year-old woman with a 6-month history of unilateral right-sided nasal obstruction and intermittent epistaxis.

A, Axial contrast-enhanced CT scan shows a calcified densely enhancing mass in the posterior ethmoidal sinuses with extension into the right orbit (courtesy of Gehring T. Sauter, MD, St Joseph Mercy Hospital, Mount Clemens, Mich).

B, Axial contrast-enhanced CT scan at a lower level shows heterogeneous enhancement of the mass in the right nasal cavity and associated benign inflammatory disease in the maxillary sinuses (courtesy of Gehring T. Sauter, MD, St Joseph Mercy Hospital, Mount Clemens, Mich).

C, Coronal CT scan shows extension of the mass through the cribriform plate and prominent central calcification (courtesy of Gehring T. Sauter, MD, St Joseph Mercy Hospital, Mount Clemens, Mich).

D, Axial noncontrast T1-weighted (550/16) MR image shows the mass to be isointense with gray matter with a central area of marked hypointensity, representing calcification.

E, Axial T2-weighted (4848/90 effective) MR image at the same level as *D* shows a mass that is hypointense relative to gray matter. Marked hypointensity of the central calcification is again seen.

F, Axial noncontrast T1-weighted (550/16) MR image at a higher level shows a homogeneous intracranial segment of the mass that is isointense with brain and extends into the frontal sinuses. Also note the mass effect on the genu of the corpus callosum and the lateral ventricles. *Figure continues.*

several weeks and she has returned to her former lifestyle without evidence of tumor 4 months after surgery.

Discussion

Solitary or localized fibrous tumor is an uncommon neoplasm that most commonly arises from the pleura (1, 2). It was described as a distinct neoplasm in 1931 by Klemperer and Rabin (1), who distinguished it from the more prevalent and aggressive diffuse malignant mesothelioma. Since then, almost 600 cases of solitary fibrous tumor of pleura have been reported. These tumors are usually round to oval and often attached to the pleura by a vascular pedicle. In two thirds of cases they arise from visceral pleura and in one third from parietal pleura. They typically occur in adults in the
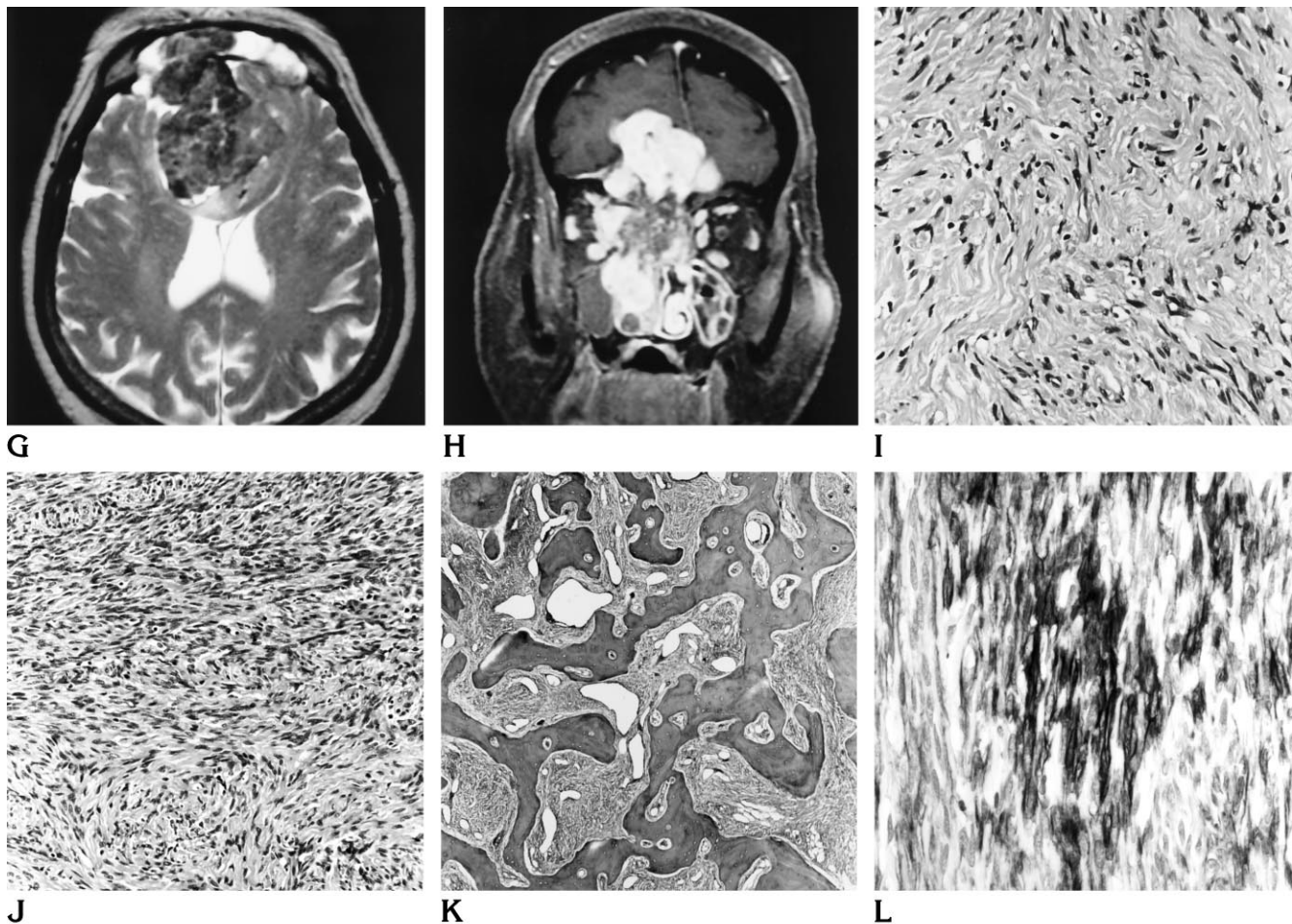
Fig 1, *continued.*

G, Axial T2-weighted (4848/90 effective) image at the same level as *F* shows the mass to be heterogeneously hypointense relative to gray matter. The intrasinus tumor is well differentiated from secretions relating to frontal sinus obstruction.

H, Coronal contrast-enhanced T1-weighted (550/16) MR image with fat suppression shows marked enhancement of the intranasal, right intraorbital, and intracranial segments of the mass. The central area of hypointensity corresponds to ossification.

I, Hypocellular region of solitary fibrous tumor, characterized by disorganized bland spindle cells and thick bands of collagen.

J, Hypercellular region of solitary fibrous tumor reveals absence of significant pleomorphism, mitotic figures, and necrosis.

K, Remodeled mature lamellar bone of the paranasal sinuses invaded by solitary fibrous tumor, corresponding to the bone seen on the radiologic images.

L, Strong CD34-positive staining of solitary fibrous tumor (fibrosarcomas are negative for CD34).

sixth and seventh decades, but the age of onset has ranged from 9 to 86 years (3).

Solitary fibrous tumors arising from the pleura are asymptomatic in approximately 50% of patients (2, 3). When symptomatic, patients present with cough, dyspnea, chest pain, pulmonary osteoarthropathy, and/or hypoglycemia (2–4). An unusual symptom of hypoglycemia relates to production of an insulinlike growth factor (IGF-1) by the tumor (5). Patients who have extrapleural tumors typically exhibit symptoms referable to the tumor's anatomic site of origin; for example, those with tumors in

the upper respiratory tract have nasal obstruction (6, 7) and those with orbital solitary fibrous tumors most commonly have unilateral proptosis (8).

In the past, solitary fibrous tumor was believed to arise from mesothelium (9), hence the designation localized fibrous mesothelioma. Recent immunohistochemical and ultrastructural studies, however, indicate that these tumors arise from a submesothelial mesenchymal fibroblastlike cell (2–4). Further, the existence of solitary fibrous tumor at extrapleural sites—including peritoneum (10), mediastinum (4, 11),

thyroid (12), thymus (4), pericardium (4, 5, 9), orbit (8), nasopharynx and paranasal sinuses (6, 7)—some of which are devoid of mesothelium, contraindicate a mesothelial origin.

Approximately 80% to 88% of pleural solitary fibrous tumors behave in a benign fashion and are cured by surgical resection. Twelve to twenty percent are associated with invasion, recurrence, and metastasis, resulting in the ultimate death of the patient (2, 3). Of eight reported cases of solitary fibrous tumor arising from the upper respiratory tract, six showed no evidence of disease on follow-up studies ranging from 1 to 12 years. One had a persistent tumor at the 4-year follow-up, and no follow-up information was available for the final patient (6, 7). Of the three patients with intraorbital solitary fibrous tumors, two had no evidence of disease at 18 months and 12 years, respectively, while the third patient had tumor recurrence at 4 years (7).

The microscopic findings in solitary fibrous tumor have commonly been described as showing a "patternless pattern" of ovoid–spindle-shaped cells with faint eosinophilic cytoplasm and nuclei with evenly distributed chromatin and small nucleoli (2, 3). The cells are randomly distributed in a background of a dense collagenous matrix. Hypercellular and sclerotic hypocellular regions characteristically alternate (4–8). Some cases have a hemangiopericyto-malike pattern of irregular branching vessels and, rarely, a storiform or herringbone pattern (3).

Primary histopathologic differential diagnostic considerations include angiofibroma, fibrous histiocytoma, spindle cell carcinoma, spindle cell melanoma, fibromatosis, fibrosarcoma, and a fibroosseous lesion, such as an ossifying fibroma. In our patient, these tumors could be excluded at light microscopy. Ossifying fibromas typically consist of fibrous connective tissue interspersed with small foci of irregular bone trabeculae that are often surrounded by osteoblasts. The neoplasm in the present case was a fibrous tumor that infiltrated mature lamellar bone that contained fatty marrow. Radiologically, ossifying fibromas generally present as destructive well-circumscribed lytic bone lesions rather than as a large soft-tissue mass.

Immunohistochemistry is a useful adjunct for differentiating other neoplasms. Van de Rijn et al (13) reported that solitary fibrous tumor is uniformly negative for keratin (carcinoma and mesothelioma are positive) and for S-100 protein (melanoma is positive). Demonstration of CD34 reactivity is a positive immunophenotype marker in 79% of solitary fibrous tumors, whereas fibrous histiocytoma, fibromatosis, fibrosarcoma, spindle cell carcinoma, and sarcomatoid mesothelioma are negative. Other studies have confirmed that fibromatoses, fibromas, and fibrosarcomas are uniformly negative for CD34 (14–16). CD34 is nonspecific, however, and is present in solitary fibrous tumors, vascular tumors, neural tumors, dermatofibrosarcoma protuberans, and others (17, 18). It is, however, useful for distinguishing fibrosarcoma from solitary fibrous tumor. Our review of the literature found one report of CD34 positivity in a fibrosarcoma (19). Goldbloom found focal staining in just one of seven fibrosarcomas arising in dermatofibrosarcoma protuberans, a fibrohistiocytic tumor that is strongly positive for CD34 (19). Thus, even when fibrosarcoma arises in a setting where it would be most expected to express CD34, it tends not to. In our case, the CD34 staining was strong and diffuse. Though this immunohistochemistry was supportive, our diagnosis was based primarily on histologic appearance. On light microscopy, low-grade fibrosarcomas are composed of long sweeping interlacing fascicles of uniform spindle cells that vary little in size and shape (20). The collagen fibers run parallel to one another and mitotic figures should be readily identifiable. The tumor described here had a disorganized, irregular pattern characteristic of solitary fibrous tumor and only focal areas that resembled fibrosarcoma. We considered these areas to indicate malignant degeneration and an increased risk for local recurrence, but not distant metastases.

The suggested pathologic criteria for the characterization of malignancy include high cellularity, more than four mitoses per 10 high-power fields, pleomorphism, hemorrhage, and necrosis (3). Approximately 45% of patients with pleural neoplasms considered malignant by the above criteria were still cured by simple surgical excision. Approximately 55% of patients with histologically malignant neoplasm succumb to their disease. Therefore, it appears that "resectability is the single most important indicator of clinical outcome" (3).

Findings of pleural solitary fibrous tumor on plain chest radiographs and CT scans are those of a well-defined lobulated mass with soft-tissue

attenuation that is located peripherally along the pleura (21–24). On occasion, they may be associated with one of the fissures and present as a mass that resembles an intraparenchymal lesion (23). On CT scans the pleural solitary fibrous tumors show inhomogeneous enhancement with an attenuation value approximately two times that of the normal surrounding muscles (24). The areas of intense enhancement represent the prominent vascularity of this tumor, while foci of low attenuation correspond to areas of myxoid or cystic degeneration and hemorrhage on histologic examination (24). Calcification is rarely present (3, 24).

In our case, the tumor presented as a large, slightly heterogeneous soft-tissue mass with a large central area of remodeled and reactive native bone that was infiltrated by the neoplasm.

The mass demonstrated MR signal characteristics that were isointense with gray matter on T1-weighted images and hypointense relative to gray matter on T2-weighted images. A central area of marked hypointensity on both T1-weighted and T2-weighted images corresponded to the prominent central area of remodeled and reactive native bone infiltrated by the neoplasm observed on CT scans as an area of bone density. Contrast-enhanced CT and MR studies showed prominent but heterogeneous enhancement. The MR signal characteristics corresponded well with the histologic findings of a fibrous stroma intermixed with prominent vascular channels.

The histologic diagnosis of malignancy in this case was based on the hypercellularity and interlacing fascicular pattern similar to that seen in low-grade fibrosarcoma, as well as the aggressive invasion through the cribriform plate into the anterior cranial fossa. The eight previously reported cases of solitary fibrous tumor involving the sinonasal cavity were all histologically benign and did not invade bone.

The differential diagnoses for a solitary fibrous tumor in the sinonasal cavity are many. They include epithelial neoplasms, esthesioneuroblastoma, aggressive meningioma, lymphoma, nasopharyngeal angiofibroma, hemangiopericytoma, schwannoma, fibromatosis, malignant fibrous histiocytoma, and fibrosarcoma (3, 6). While each of these tumors can demonstrate a spectrum of signal intensities on T1- and T2-weighted MR images, the most common pattern is that of hypointensity to isointensity on T1-weighted images, heterogeneous hyperintensity on T2-weighted images, and a variable degree of pathologic contrast enhancement (25–34).

The tumor in our case showed predominantly hypointense signal intensity on T2-weighted images, unlike the hyperintensity typical of the more common soft-tissue neoplasms of the sinonasal cavity. Another interesting attribute of the present case was the presence of a significantly remodeled mature native bone within the tumor in the region of the ethmoidal sinuses and cribriform plate. In the sinonasal cavity, ossifications or calcifications can be seen with osteosarcomas and chondrosarcomas, both of which are rare tumors in this region (25). Ossification associated with malignant fibrous histiocytomas and esthesioneuroblastomas have also been reported (29, 34). Along with a partly calcified meningioma with extension into the sinonasal cavity, all these neoplasms may be difficult to distinguish, by radiologic appearance alone, from solitary fibrous tumor containing remodeled and infiltrated mature native bone, as seen in the present case.

In conclusion, our findings suggest that in a patient with a neoplasm of the sinonasal cavity that shows irregular central bone density on CT scans and isointensity to hypointensity of the soft-tissue component on T2-weighted MR images, solitary fibrous tumor should be included in the differential diagnosis.

References

1. Klemperer P, Rabin CB. Primary neoplasms of the pleura. A report of five cases. *Arch Pathol* 1931;11:385–412
2. Briselli M, Mark EJ, Dickersin GR. Solitary fibrous tumors of the pleura: eight new cases and review of 360 cases in the literature. *Cancer* 1981;47:2678–2689
3. England DM, Hochholzer L, McCarthy MJ. Localized benign and malignant fibrous tumors of the pleura: a clinicopathologic review of 223 cases. *Am J Surg Pathol* 1989;13:640–658
4. Witkin GB, Rosai J. Solitary fibrous tumor of the mediastinum: a report of 14 cases. *Am J Surg Pathol* 1989;13:547–557
5. Bortolotti U, Calabrò F, Loy M, Fasoli G, Altavilla G, Marchese D. Giant intrapericardial solitary fibrous tumor. *Ann Thorac Surg* 1992;54:1219–1220
6. Zukerberg LR, Rosenberg AE, Randolph G, Pilch BZ, Goodman ML. Solitary fibrous tumor of the nasal cavity and paranasal sinuses. *Am J Surg Pathol* 1991;15:126–130
7. Witkin GB, Rosai J. Solitary fibrous tumor of the upper respiratory tract: a report of six cases. *Am J Surg Pathol* 1991;15:842–848
8. Dorfman DM, To K, Dickersin GR, Rosenberg AE, Pilch BZ. Solitary fibrous tumor of the orbit. *Am J Surg Pathol* 1994;18:281–287

9. Stout AP, Himadi GM. Solitary (localized) mesothelioma of the pleura. *Ann Surg* 1951;133:50–64

10. Young RH, Clement PB, McCaughey WTE. Solitary fibrous tumors (fibrous mesotheliomas) of the peritoneum. *Arch Pathol Lab Med* 1990;114:493–495

11. Weidner N. Solitary fibrous tumor of the mediastinum. *Ultrastruct Pathol* 1991;15:489–492

12. Cameselle-Teijeiro J, Varela-Durá n, Fonseca E, Villanueva JP, Sobrinho-Simoes M. Solitary fibrous tumor of the thyroid. *Am J Clin Pathol* 1994;101:535–538

13. Van de Rijn M, Lombard CM, Rouse RV. Expression of CD34 by solitary fibrous tumors of the pleura, mediastinum and lung. *Am J Surg Pathol* 1994;18:814–820

14. Mechtersheimer G. Towards the phenotyping of soft tissue tumors by cell surface molecules. *Virchows Arch A Pathol Anat Histopathol* 1991;419:7–28

15. Kutzner H. Expression of the human progenitor cell antigen CD34 (HPCA-1) distinguishes dermatofibrosarcoma protuberans from fibrous histiocytoma in formalin-fixed, paraffin embedded tissue. *J Am Acad Dermatol* 1993;28:613–617

16. Aiba S, Tabata N, Ishii H, Ootani H, Tagami H. Dermatofibrosarcoma protuberans is a unique fibrohistiocytic tumor expressing CD34. *Br J Dermatol* 1992;127:79–84

17. Traweek ST, Kandalaft PL, Mehta P, Battifora H. The human hematopoietic progenitor cell antigen (CD34) in vascular neoplasia. *Am J Clin Pathol* 1991;96:25–31

18. Weiss SW, Nickoloff BJ. CD34 is expressed by a distinctive cell population in peripheral nerve, nerve sheath tumors, and related lesions. *Am J Surg Pathol* 1993;17:1039–1045

19. Goldbloom JR. CD34 positivity in fibrosarcomas which arise in dermatofibrosarcoma protuberans. *Arch Pathol Lab Med* 1995; 119:238–241

20. Enzinger FM, Weiss SW. *Soft Tissue Tumors.* St Louis, Mo: Mosby; 1995

21. Blount HC Jr. Localized mesothelioma of the pleura. *Radiology* 1956;67:822–833

22. Dedrick CG, McLoud TC, Shepard JO, Shipley RT. Computed tomography of localized pleural mesothelioma. *AJR Am J Roentgenol* 1985;144:275–280

23. Spizarny DL, Gross BH, Shepard JO. CT findings in localized fibrous mesothelioma of the pleural fissure. *J Comput Assist Tomogr* 1986;10:942–944

24. Lee KS, Im J-G, Choe KO, Kim CJ, Lee BH. CT findings in benign fibrous mesothelioma of the pleura: pathologic correlation in nine patients. *AJR Am J Roentgenol* 1992;158:983–986

25. Curtin HD, Hirsch WL. Base of the skull. In: Atlas S, ed. *Magnetic Resonance Imaging of the Brain and Spine.* New York, NY: Raven Press; 1991:669–707

26. Som PM, Dillon WP, Sze G, Lidov M, Biller HF, Lawson W. Benign and malignant sinonasal lesions with intracranial extension: differentiation with MR imaging. *Radiology* 1989;172:763–766

27. Elster AD, Challa VR, Gilbert TH, Richardson DN, Contento JC. Meningiomas: MR and histopathologic features. *Radiology* 1989; 170:857–862

28. Kransdorf MJ, Jelinek JS, Moser RP Jr, et al. Magnetic resonance appearance of fibromatosis: a report of 14 cases and review of the literature. *Skeletal Radiol* 1990;19:495–499

29. Miller TT, Hermann G, Abdelwahab IF, Klein MJ, Kenan S, Lewis MM. MRI of malignant fibrous histiocytoma of soft tissue: analysis of 13 cases with pathologic correlation. *Skeletal Radiol* 1994;23: 271–275

30. Li C, Yousem DM, Hayden RE, Doty RL. Olfactory neuroblastoma: MR evaluation. *AJNR Am J Neuroradiol* 1993;14:1167–1171

31. Lorigan JG, David CL, Evans HL, Wallace S. The clinical and radiologic manifestations of hemangiopericytoma. *AJR Am J Roentgenol* 1989;153:345–349

32. Chin LS, Rabb CH, Hinton DR, Apuzzo MLJ. Hemangiopericytoma of the temporal bone presenting as a retroauricular mass. *Neurosurgery* 1993;33:728–731

33. Cosentino CM, Poulton TB, Esguerra JV, Sands SF. Giant cranial hemangiopericytoma: MR and angiographic findings. *AJNR Am J Neuroradiol* 1993;14:253–256

34. Regenbogen VS, Zinreich SJ, Kim KS, et al. Hyperostotic esthesioneuroblastoma: CT and MR findings. *J Comput Assist Tomogr* 1988;12:52–56